

ANALYSIS AND EFFICIENT ESTIMATION OF RANDOM WIRE BUNDLES EXCITED BY PLANE-WAVE FIELDS

H. Xie^{1,*}, J. Wang², S. Li¹, H. Qiao¹, and Y. Li¹

¹Northwest Institute of Nuclear Technology, P. O. Box 69-12, Xi'an, Shaanxi 710024, China

²Northwest Institute of Nuclear Technology, P. O. Box 69-1, Xi'an, Shaanxi 710024, China

Abstract—The random wire bundle is an important factor resulting in the randomness of the interferences. This paper studies the effect of random wire positions due to the bundle rotation on the coupling with external fields and presents an efficient method to estimate the averages and standard deviations of the voltages and powers induced on the loads. Three configurations of a four-wire bundle under external fields are investigated by using the Baum-Liu-Tesche equation in the frequency domain and together with the inverse Fourier transform in the time domain, and the results show that the induced voltages and powers change as sine functions when the bundle rotates. The proposed method can estimate the averages and standard deviations of the induced voltages and powers quickly, just by three times repeated analysis, and the results agree well with those obtained statistically.

1. INTRODUCTION

External electromagnetic pulse (EMP) can disturb electronic systems, which draws much attention. However, because the positions of wires, cables, and devices inside electronic systems are not definitive, the interferences on electronic systems have randomness. As a result, any deterministic solution is not sufficient for the assessment of system performance under external threats. The randomness of wire bundles is an important factor resulting in the randomness of the interferences and the study of EMP coupling to random wires is important.

Received 15 September 2011, Accepted 17 October 2011, Scheduled 24 October 2011

* Corresponding author: Haiyan Xie (xiehy05@mails.tsinghua.edu.cn).

Lots of researches have been done on external EMPs coupling to wires or cables in the frequency or time domain [1–12]. In these researches, the positions and geometries of wires or cables are specified exactly. Some researchers have paid some attention on the effect due to the uncertainties of wire or cable positions. Capraro et al. studied the crosstalk sensitivity to the uncertainties of the wire positions in a multiwire bundle by statistical analysis of the experimental data [13]. Ciccolella and Canavero used the Monte Carlo method to describe the geometry and the multiconductor transmission line theory to predict the crosstalk of a random cable [14]. After 2000, more and more study has been done on this topic and different models and methods have been proposed [15–20]. However, these researches are mainly focused on the crosstalk variation due to the random wire positions, but without consideration of external fields.

Random wire positions' effect on fields coupling is more complicated to analyze than that on crosstalk and much less study has been done on this topic. Morgan et al. proposed a technique for external fields induced to an n -wire random cable by the reciprocity theorem and a representation of a statistical ensemble; however, no numerical examples were given [21]. Afterwards, Parkinson et al. investigated statistically an EMP response of a random-lay cable, where the cable was represented as multisegment lines with random connections between adjacent segments [22]. Recently, Nuno and Holloway studied statistically the induced voltage on a random position cable inside a cavity by using the finite-difference time domain method [23]. In the study by Paletta et al., external fields interaction with wiring in a complex system, the random positions of the wires in bundles were taken into account, but the random wire positions' influence on the coupling was not studied and the transmission line parameters were calculated just by averaging the parameters of several cross-sections [24].

Because wire bundles may rotate around the axis and the cross section will change, as seen in [24], this paper aims at studying the effect of bundle rotation on the coupling statistically by using the Baum-Liu-Tesche (BLT) equation [25, 26], and then puts forward an efficient method to estimate the averages and standard deviations of the induced voltages and powers.

This paper is organized as follows. Section 2 presents the analysis method and Section 3 establishes the models to be analyzed and gives numerical results. Based on the results, the efficient estimation method is proposed in Section 4. At last, conclusions are made in Section 5.

2. COMPUTATION AND ANALYSIS METHOD

The BLT equation, based on the transmission line theory, is adopted to compute the terminal responses of wire bundles excited by external plane-wave fields in the frequency domain. The BLT equation is derived from the propagation and scattering equations and can be expressed as [26]

$$\hat{\mathbf{V}} = (\mathbf{U} + \hat{\rho}) \cdot \left(-\hat{\rho} + \hat{\Gamma}\right)^{-1} \cdot \hat{\mathbf{S}}, \tag{1}$$

where $\hat{\mathbf{V}} = [\hat{\mathbf{V}}(0), \hat{\mathbf{V}}(L)]^T$ is the terminal voltage complex vector and consists of voltage vectors at the near and far ends, with L the length of the bundle. $\hat{\cdot}$ represents complex quantities. \mathbf{U} is the unit matrix. $\hat{\rho} = \text{diag}(\hat{\rho}_1, \hat{\rho}_2)$ is the scattering matrix, where $\hat{\rho}_1$ and $\hat{\rho}_2$ are the reflecting coefficient matrix at the near and far ends, respectively. The propagation matrix $\hat{\Gamma}$ is the function matrix of the propagation constant and the bundle length. $\hat{\mathbf{S}}$ is a vector related to the excitation fields and, according to the Agrawal's model [2], can be written as

$$\hat{\mathbf{S}} = \begin{bmatrix} \frac{1}{2} \int_0^L e^{\hat{\gamma}z} \hat{\mathbf{V}}'_s(z) dz - \frac{1}{2} \hat{\mathbf{V}}_{s1} + \frac{1}{2} e^{\hat{\gamma}L} \hat{\mathbf{V}}_{s2} \\ -\frac{1}{2} \int_0^L e^{\hat{\gamma}(L-z)} \hat{\mathbf{V}}'_s(z) dz + \frac{1}{2} e^{\hat{\gamma}L} \hat{\mathbf{V}}_{s1} - \frac{1}{2} \hat{\mathbf{V}}_{s2} \end{bmatrix}, \tag{2}$$

where $\hat{\mathbf{V}}'_s(z)$ is distributed voltage source along the bundle and $\hat{\mathbf{V}}_{s1}(z)$ and $\hat{\mathbf{V}}_{s2}(z)$ are lumped voltage sources at the ends generated by external fields.

Equation (2) implies that even for a very simple random bundle it is difficult to study the coupling variation analytically and thus the statistical method is applied. The rotation angle, with the definition given in Figure 1, is assumed to be uniformly distributed in the range of $[0, 2\pi]$ and N samples of the rotation angles are selected. For each angle

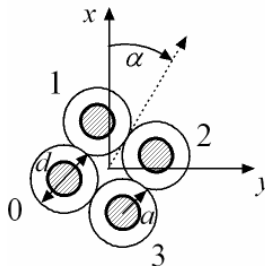


Figure 1. Cross section of the four-wire bundle and definition of the rotation angle.

sample, the voltages on the terminal loads are computed by using the BLT equation in the frequency domain and together with the inverse Fourier transform (IFT) in the time domain, and then the averages and standard deviations of the voltages and powers on the loads are estimated statistically.

3. MODELS AND NUMERICAL RESULTS

A four-wire bundle with the length 1.0m excited by a plane-wave electromagnetic field is studied. Figure 1 shows the cross section of the four-wire bundle. The four wires with radius $r_0 = 0.68$ mm are insulated with each other. The diameter of the insulators d is 1.36 mm. In order to study the rotation effect on the coupling of electromagnetic fields to the bundle, three different configurations of the bundle are considered, as shown in Table 1. The four-wire bundles in case 2 and case 3 are over the infinite and perfectly conducting ground with the height $h = 10.0$ mm. Case 1 and case 2 have terminal connection 1 while case 3 has terminal connection 2. The details of the terminal connections are given in Table 2, with all resistances 50Ω . In terminal connection 1, the wire 1, wire 2, and wire 3 are connected to the wire 0 by resistances R_{i1} , R_{i2} , and R_{i3} at both the ends of the bundle ($i = 1$ at the near end and $i = 2$ at the far end), respectively, but while in terminal connection 2, all the four wires are connected to the ground by 50Ω resistances at both the ends. The sample number N is set to

Table 1. Three cases of the four-wire bundle.

	Ground	Terminal connection
Case 1	Without the ground	Terminal connection 1
Case 2	With the ground	Terminal connection 1
Case 3	With the ground	Terminal connection 2

Table 2. Two different terminal connections ($i = 1$ at the near end and $i = 2$ at the far end).

	Terminal connection 1	Terminal connection 2
	Wire 0	Ground
Wire 0	\times	R_{i0}
Wire 1	R_{i1}	R_{i1}
Wire 2	R_{i2}	R_{i2}
Wire 3	R_{i3}	R_{i3}

30.

The plane-wave electromagnetic field of oblique incidence is considered and the incident angles are $\theta_p = 45^\circ$, $\varphi_p = -60^\circ$, and $\theta_E = 90^\circ$, respectively, with the definitions shown in Figure 2.

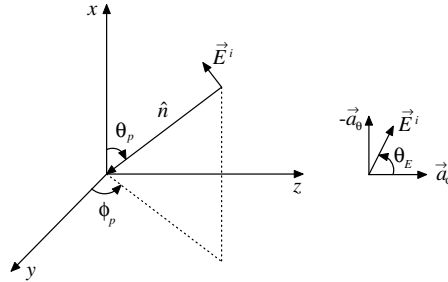


Figure 2. Definitions of the incident angles of the plane-wave electromagnetic field.

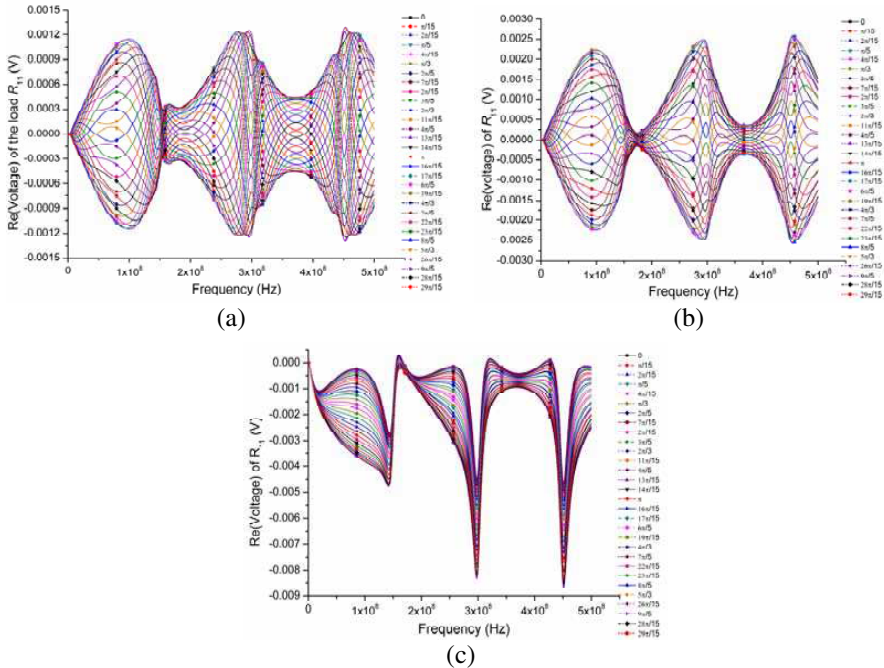


Figure 3. The real part of the voltage induced on R_{11} . (a) Case 1. (b) Case 2. (c) Case 3.

3.1. Frequency Domain Analysis

The incident wave of the unit electric field is applied for the frequency domain analysis. For each sample, the voltages and powers of the loads induced by external fields are computed by using the BLT equation. Figure 3 shows the real parts of the voltage \hat{V}_{11} on the load R_{11} in the three cases. In case 1 and case 2, the curves of the $\text{Re}(\hat{V}_{11})$ with different rotation angles are symmetric around the $y = 0$, so the averages of $\text{Re}(\hat{V}_{11})$ in cases 1 and 2 are zero. In case 1, the configuration has not the ground and relatively positions of the wires do not change with the rotation angle, so the per-unit-length (p.u.l.) parameters, such as capacitance and inductance, do not change with the rotation angle. As a result, only the term $\hat{\mathbf{S}}$ in (1) changes with the angle α . In cases 2 and 3, not only the term $\hat{\mathbf{S}}$ but also the p.u.l. parameters change with the angle α because of the ground. Thus, it is difficult to conjecture the trend of the induced voltages changing with

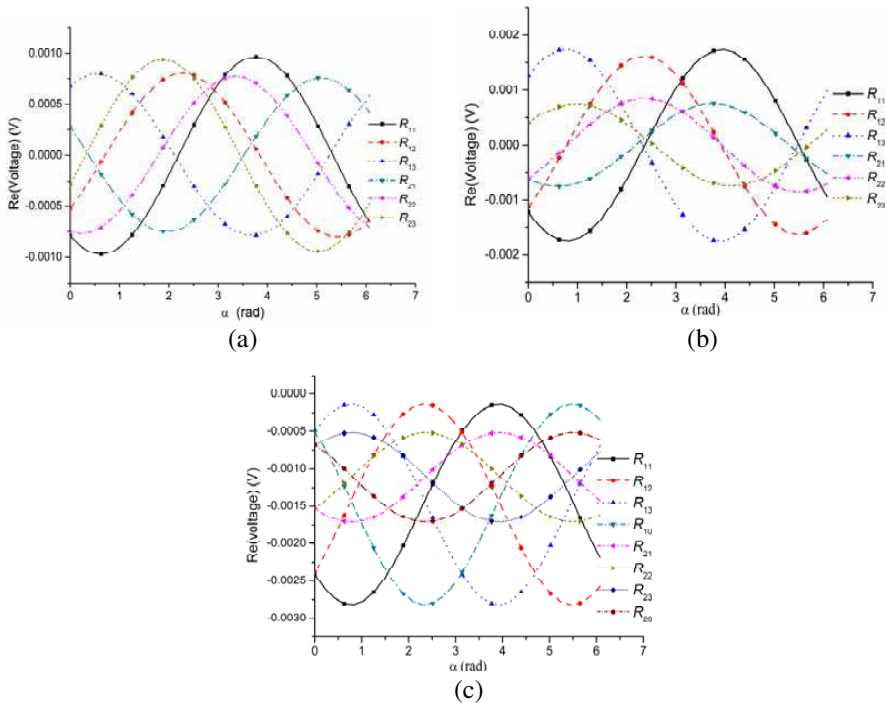


Figure 4. The real parts of the induced voltages at 250 MHz. (a) Case 1. (b) Case 2. (c) Case 3.

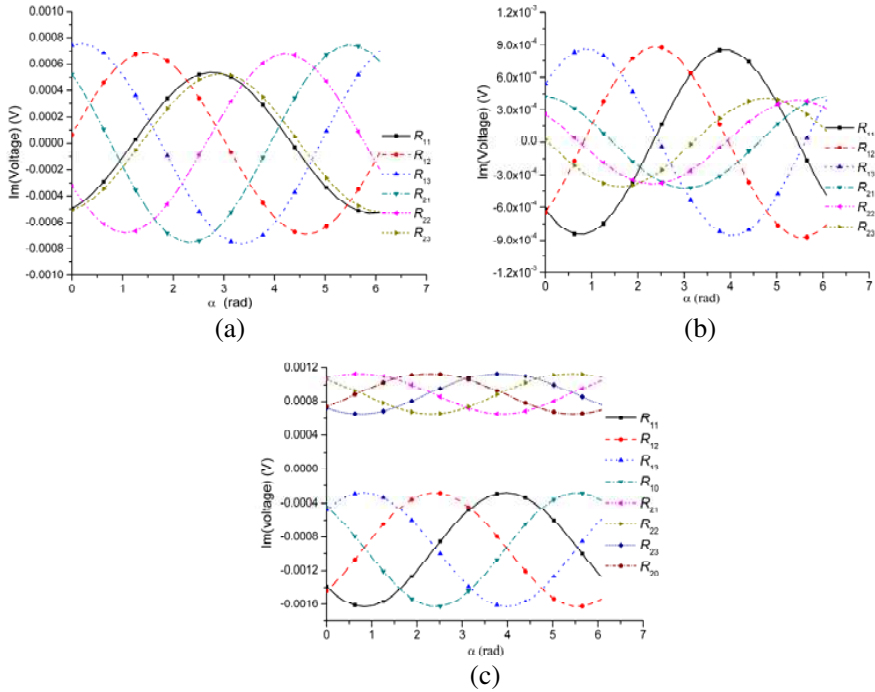


Figure 5. The imaginary parts of the induced voltages at 250 MHz. (a) Case 1. (b) Case 2. (c) Case 3.

the angle α directly.

To get the trend of the induced voltages when the bundle rotates, Figures 4 and 5 show the real and imaginary parts of the induced voltages changing with the rotation angle α at 250 MHz, respectively. It can be tentatively concluded that both the real and imaginary parts of all the induced voltages are sine functions of the rotation angle α with cycle 2π whatever the ground exists or the bundle has different terminal connections. To validate this conclusion, Figure 6 shows the comparison between the induced voltage \hat{V}_{11} and the sine functions, whose parameters are listed in Table 3, and they agree well with each other.

Figure 7 shows the standard deviations of the real and imaginary parts of the induced voltages in case 1. The induced power P is an important quantity in the EMP effect analysis and can be computed from the induced voltage \hat{V} by the expression

$$P(\omega) = \frac{1}{2R} \left| \hat{V}(\omega) \right|^2. \quad (3)$$

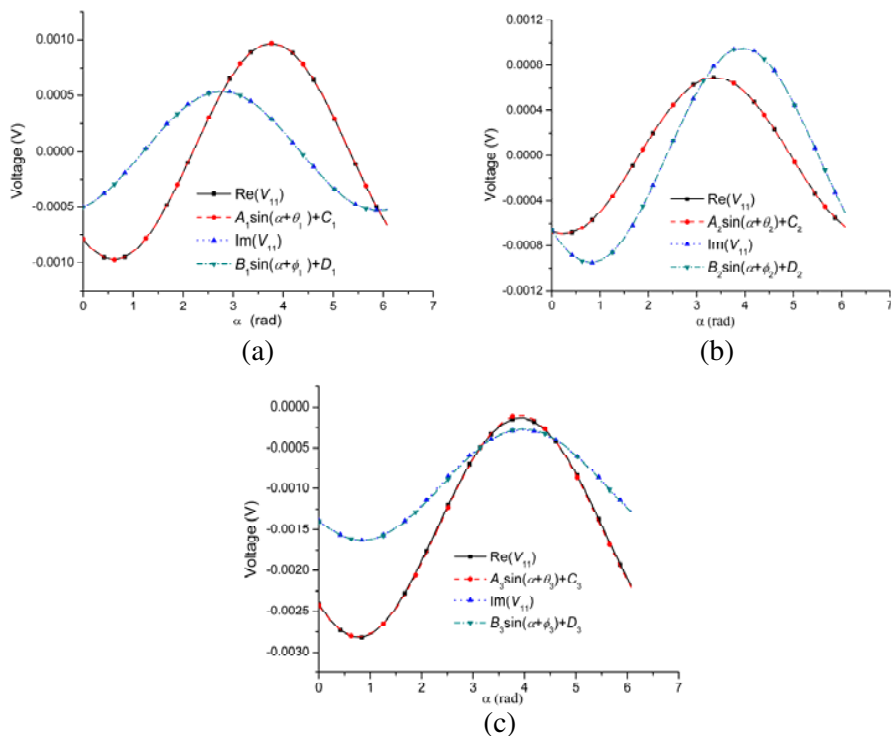


Figure 6. The comparison between the voltage \hat{V}_{11} and the sine functions at 250 MHz. (a) Case 1. (b) Case 2. (c) Case 3.

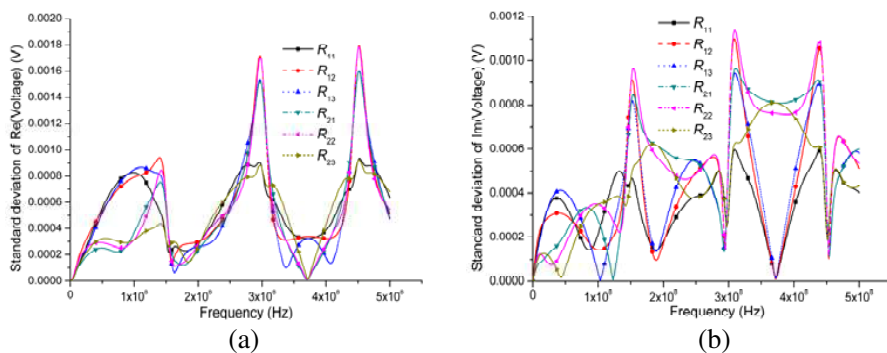


Figure 7. The standard deviations of the real and imaginary parts of the induced voltages in case 1. (a) Standard deviations of the real parts. (b) Standard deviations of the imaginary parts.

Table 3. The values of the parameters in the sine functions.

	A_i	θ_i	C_i	B_i	Φ_i	D_i
Case 1 ($i = 1$)	9.71×10^{-4}	4.09	0.00	5.35×10^{-4}	-1.20	0.00
Case 2 ($i = 2$)	6.94×10^{-4}	4.48	0.00	9.54×10^{-4}	3.91	0.00
Case 3 ($i = 3$)	13.5×10^{-4}	3.94	-14.6×10^{-4}	6.80×10^{-4}	3.87	-9.47×10^{-4}

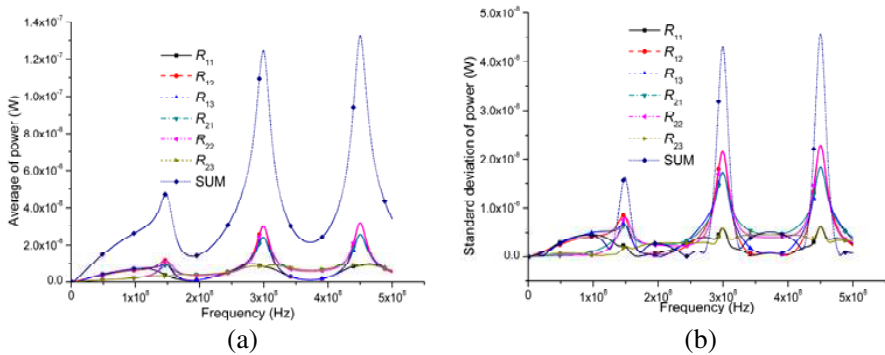


Figure 8. The averages and standard deviations of the induced powers obtained statistically. (a) Averages. (b) Standard deviations.

Figure 8 shows the averages and standard deviations of each load’s induced power and the total induced power, which is the sum of the powers induced on all the loads, in the first configuration. The results indicate that each load’s induced power’s standard deviation is of the similar size with its average; however, the total induced power’s standard deviation is much smaller than its average. This means that single load’s induced power rather than the total induced power can reach zero when the bundle rotates. Figure 9, which shows each load’s induced power and the total induced power change with the rotation angle α at the frequency of 250 MHz, proves this conclusion. Since the induced voltage is the sine function of the rotation angle α , the induced power is also the sine function of the angle α , but with the cycle of π , as shown in Figure 9.

3.2. Time Domain Analysis

The incident wave modeled by the biexponential pulse $E_0(t) = kE_0[\exp(-\beta t) - \exp(-\alpha t)]$, where $k = 1.3$, $E_0 = 50 \text{ kV/m}$, $\alpha =$

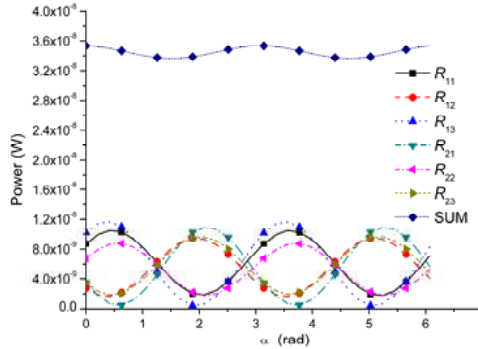


Figure 9. Each load’s induced power and the total power change with the angle α at 250 MHz.

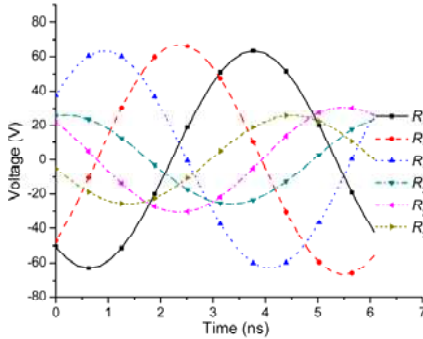


Figure 10. The transient induced voltages at 5 ns in case 2.

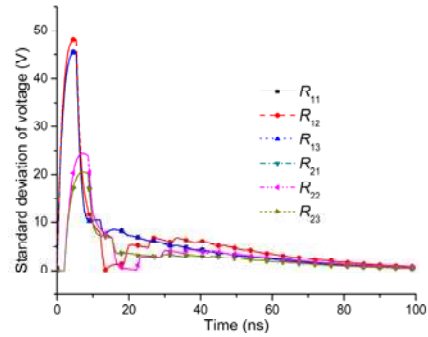


Figure 11. The standard deviations of the induced voltages in case 2.

$6.0 \times 10^8 \text{ s}^{-1}$, and $\beta = 4.0 \times 10^7 \text{ s}^{-1}$, is used for the time domain analysis. For each sample, the voltages and powers induced on the loads in the time domain are computed by using the BLT equation together with IFT. Because the real and imaginary parts of the induced voltage are the sine functions of the rotation angle α in the frequency domain analysis, it is not difficult to get that the transient induced voltage V is also the sine function of the rotation angle α . Figure 10 shows the induced voltage on each load in case 2 at the time of 5 ns. In this configuration, the induced voltages on all the loads are sine functions of the angle α with the cycle of 2π and the average about 0. The standard deviations of all the loads’ induced voltages computed statistically are shown in Figure 11.

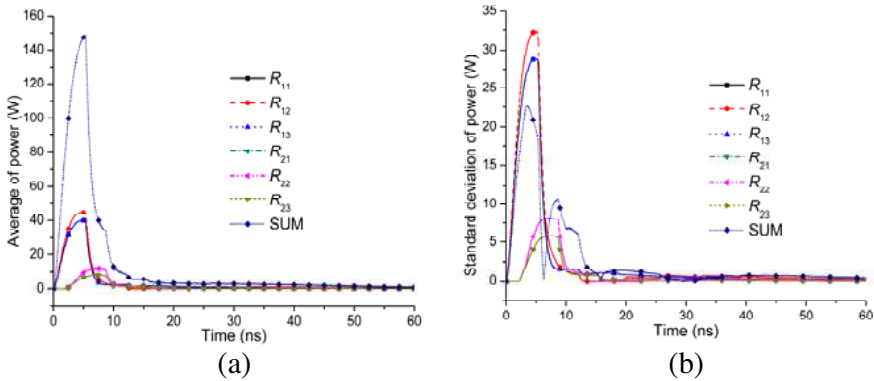


Figure 12. The averages and standard deviations of the induced powers in case 2. (a) Averages. (b) Standard deviations.

The induced power P can be easily calculated by using the expression $P(t) = V^2(t)/R$. Then the averages and standard deviations of each load’s power and the total power can be computed statistically and are shown in Figure 12. The results imply that the total induced power has the maximum average 148.7 W at 5.3 ns, when the standard deviation is 18.9 W.

4. EFFICIENT ESTIMATION METHOD

In Section 4, the effect of the bundle rotation on the external fields coupling to the wire bundle has been studied and the averages and standard deviations of the induced voltages and powers have been estimated statistically. However, the estimation of the averages and standard deviations by the statistical analysis takes lots of computation, attributed to the need to compute N samples of the wire bundle. In order to estimate the averages and standard deviations of the induced voltages and powers quickly, an efficient estimation method is put forward.

4.1. Estimation in the Frequency Domain

From the above analysis, the real and imaginary parts of the induced voltages on all the loads are the sine functions of the rotation angle α , so the i th load’s induced voltage \hat{V}_i can be expressed as

$$\hat{V}_i(\alpha, \omega) = A_i(\omega) \sin(\alpha + \theta_i(\omega)) + C_i(\omega) + j [B_i(\omega) \sin(\alpha + \phi_i(\omega)) + D_i(\omega)] \tag{4}$$

where $A_i(\omega)$, $\theta_i(\omega)$, $C_i(\omega)$, $B_i(\omega)$, $\varphi_i(\omega)$, and $D_i(\omega)$ are unknown quantities to be determined. From (4), we have

$$\hat{V}_i(\alpha + \pi/2, \omega) = A_i(\omega) \cos(\alpha + \theta_i(\omega)) + C_i(\omega) + j [B_i(\omega) \cos(\alpha + \phi_i(\omega)) + D_i(\omega)] \quad (5)$$

$$\hat{V}_i(\alpha + \pi, \omega) = -A_i(\omega) \sin(\alpha + \theta_i(\omega)) + C_i(\omega) + j [-B_i(\omega) \sin(\alpha + \varphi_i(\omega)) + D_i(\omega)]. \quad (6)$$

Combing (4) with (6) yields

$$C_i = \frac{1}{2} \text{Re} [\hat{V}_i(\alpha) + \hat{V}_i(\alpha + \pi)] \quad (7)$$

$$D_i = \frac{1}{2} \text{Im} [\hat{V}_i(\alpha) + \hat{V}_i(\alpha + \pi)]. \quad (8)$$

From (4) and (5), A_i and B_i can be written as

$$A_i = \sqrt{(\text{Re}(\hat{V}_i(\alpha)) - C_i)^2 + (\text{Re}(\hat{V}_i(\alpha + \pi/2)) - C_i)^2} \quad (9)$$

$$B_i = \sqrt{(\text{Im}(\hat{V}_i(\alpha)) - D_i)^2 + (\text{Im}(\hat{V}_i(\alpha + \pi/2)) - D_i)^2}. \quad (10)$$

Then $\sin(\alpha + \theta_i)$ and $\cos(\alpha + \theta_i)$ can be obtained by

$$\sin(\alpha + \theta_i) = (\text{Re}(\hat{V}_i(\alpha)) - C_i) / A_i \quad (11)$$

$$\cos(\alpha + \theta_i) = (\text{Re}(\hat{V}_i(\alpha + \pi/2)) - C_i) / A_i. \quad (12)$$

If $\cos(\alpha + \theta_i) \geq 0$, then

$$\theta_i = \arcsin\left(\frac{1}{A_i} (\text{Re}(\hat{V}_i(\alpha)) - C_i)\right) - \alpha. \quad (13)$$

Otherwise,

$$\theta_i = \pi - \arcsin\left(\frac{1}{A_i} (\text{Re}(\hat{V}_i(\alpha)) - C_i)\right) + \alpha \quad (14)$$

The angle ϕ_i can be computed similarly. The above equations imply that the unknown quantities A_i , θ_i , C_i , B_i , ϕ_i , and D_i can be determined with the values of $\hat{V}_i(\alpha)$, $\hat{V}_i(\alpha + \pi/2)$, and $\hat{V}_i(\alpha + \pi)$, where the angle α can be any value in $[0, 2\pi]$ and is set to 0 for convenience. This implies that the induced voltage \hat{V}_i can be determined once $\hat{V}_i(0)$, $\hat{V}_i(\pi/2)$, and $\hat{V}_i(\pi)$ are computed and only 3 rather than N samples of the wire bundle have to be computed.

The rotation angle α is uniformly distributed in $[0, 2\pi]$, so the average and standard deviation of the function $y(\alpha)$ can be computed by

$$\langle y(\alpha) \rangle = \frac{1}{2\pi} \int_0^{2\pi} y(\alpha) d\alpha \tag{15}$$

$$\sigma(y(\alpha)) = \sqrt{\frac{1}{2\pi} \int_0^{2\pi} (y(\alpha) - \langle y \rangle)^2 d\alpha} = \sqrt{\langle y^2 \rangle - \langle y \rangle^2}. \tag{16}$$

With (4), (15), and (16), the induced voltage's average and the real and imaginary parts' standard deviation can be written as,

$$\langle \hat{V}_i \rangle = C_i + jD_i \tag{17}$$

$$\sigma \left(\text{Re} \left(\hat{V}_i \right) \right) = A_i / \sqrt{2} \tag{18}$$

$$\sigma \left(\text{Im} \left(\hat{V}_i \right) \right) = B_i / \sqrt{2} \tag{19}$$

By Equation (3), the average and standard deviation of the induced power can be computed and are given by

$$\langle P_i \rangle = \frac{1}{4R_i} (A_i^2 + B_i^2 + 2C_i^2 + 2D_i^2) \tag{20}$$

$$\begin{aligned} \sigma(P_i) = \frac{1}{4R_i} \left\{ 2[A_i B_i \cos(\theta_i - \phi_i) + 4C_i D_i]^2 - 32C_i^2 D_i^2 \right. \\ \left. + \frac{1}{2} (A_i^4 + B_i^4) + 8(A_i^2 C_i^2 + B_i^2 D_i^2) - A_i^2 B_i^2 \right\}^{1/2} \end{aligned} \tag{21}$$

Then the average and standard deviation of the total induce power P_t are given by

$$\langle P_t \rangle = \sum_{i=1}^n \frac{1}{4R_i} (A_i^2 + B_i^2 + 2C_i^2 + 2D_i^2) \tag{22}$$

$$\begin{aligned} D(P_t) = \sum_{i=1}^n \sum_{k=1}^n \frac{1}{16R_i R_k} \left\{ [A_i A_k \cos(\theta_i - \theta_k) + 4C_i C_k]^2 - \frac{A_i^2 A_k^2}{2} - 16C_i^2 C_k^2 \right. \\ + [A_i B_k \cos(\theta_i - \phi_k) + 4C_i D_k]^2 - \frac{A_i^2 B_k^2}{2} - 16C_i^2 D_k^2 \\ + [B_i A_k \cos(\phi_i - \theta_k) + 4D_i C_k]^2 - \frac{B_i^2 A_k^2}{2} - 16D_i^2 C_k^2 \\ \left. + [B_i B_k \cos(\phi_i - \phi_k) + 4D_i D_k]^2 - \frac{B_i^2 B_k^2}{2} - 16D_i^2 D_k^2 \right\} \end{aligned} \tag{23}$$

$$\sigma(P_t) = \sqrt{D(P_t)}, \tag{24}$$

where $D(P_t)$ is the variance of the total induced power.

The induced voltage vector $\hat{\mathbf{V}}$ in case 1 is computed first when the rotation angle α is 0, $\pi/2$, or π . Then the above method is used to estimate the standard deviations of the real and imaginary parts of the induced voltages and the results are shown in Figure 13, which are in a good agreement with Figure 7.

Figure 14 shows the averages and standard deviations of all the loads' power and the induced powers obtained by the Equations (20) ~ (24), and agrees well with Figure 8.

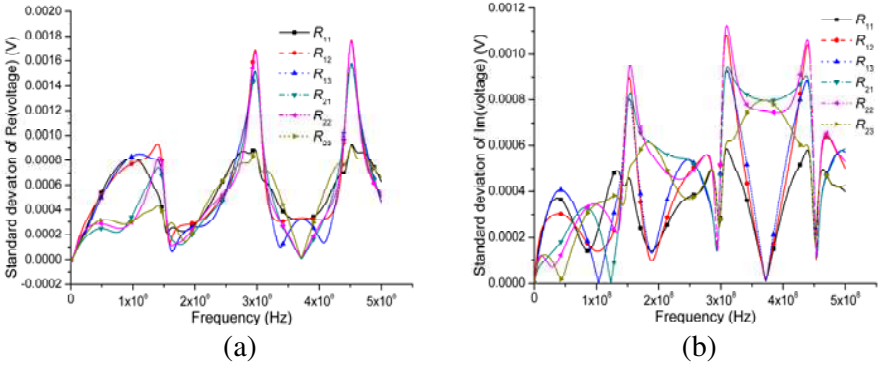


Figure 13. Standard deviations of the real and imaginary parts of the induced voltages in case 1 obtained by the proposed method. (a) Standard deviations of the real parts. (b) Standard deviations of the imaginary parts.

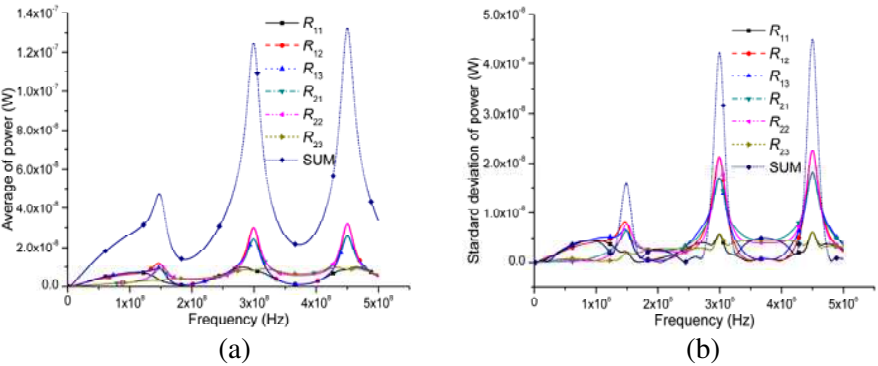


Figure 14. The averages and standard deviations of the powers in case 1 are estimated by using the efficient method. (a) Averages. (b) Standard deviations.

4.2. Estimation in the Time Domain

The induced voltages in the time domain are also the sine function of the angle α . However, the expressions of the induced voltages in the time domain are much simpler than those in the frequency domain, because the induced voltages in the time domain have no imaginary parts. As a result, the i th load's voltage V_i can be written as

$$V_i(\alpha, t) = M_i(t) \sin(\alpha + \varphi_i(t)) + N_i(t) \quad (25)$$

where M_i , φ_i , and N_i are unknown quantities to be determined. Similarly as in the frequency domain, M_i , φ_i , and N_i can be determined once $V_i(0)$, $V_i(\pi/2)$, and $V_i(\pi)$ are computed. If SPICE models for transmission lines excited by external fields are used to compute the induced voltages in the time domain directly [4, 27], M_i , φ_i , and N_i can be determined very quickly.

The quantities M_i , φ_i , and N_i can be calculated by the following equations,

$$N_i = (V_i(0) + V_i(\pi)) / 2 \quad (26)$$

$$M_i = \sqrt{(V_i(0) - N_i)^2 + (V_i(\pi/2) - N_i)^2} \quad (27)$$

$$\sin(\varphi_i) = (V_i(0) - N_i) / M_i \quad (28)$$

$$\cos(\varphi_i) = (V_i(\pi/2) - N_i) / M_i. \quad (29)$$

If $V_i(\pi/2) - N_i \geq 0$, then

$$\varphi_i = \arcsin((V_i(0) - N_i) / M_i); \quad (30)$$

Otherwise,

$$\varphi_i = \pi - \arcsin((V_i(0) - N_i) / M_i) \quad (31)$$

With (15) and (16), the averages and standard deviations of the induced voltages and powers can be written as

$$\langle V_i \rangle = N_i \quad (32)$$

$$\sigma(V_i) = M_i / \sqrt{2} \quad (33)$$

$$\langle P_i \rangle = \frac{1}{2R_i} (M_i^2 + 2N_i^2) \quad (34)$$

$$\sigma(P_i) = \sqrt{D(P_i)} = \frac{M_i^2}{2\sqrt{2}R_i} \sqrt{M_i^2 + 16N_i^2} \quad (35)$$

$$\langle P_t \rangle = \sum_{i=1}^n \frac{1}{2R_i} (M_i^2 + 2N_i^2) \quad (36)$$

$$\begin{aligned} \sigma(P_t) &= \sqrt{D(P_t)} \\ &= \sqrt{\sum_{i=1}^n \sum_{k=1}^n \frac{1}{8R_i R_k} \left\{ 2[M_i M_k \cos(\varphi_i - \varphi_k) + 4N_i N_k]^2 - 32N_i^2 N_k^2 - M_i^2 M_k^2 \right\}} \end{aligned} \quad (37)$$

Figure 15 shows the standard deviations of the induced voltages in case 2 obtained by the proposed method. The results agree well with those in Figure 11, but take much less time than the statistical method does. The averages and standard deviations of the induced

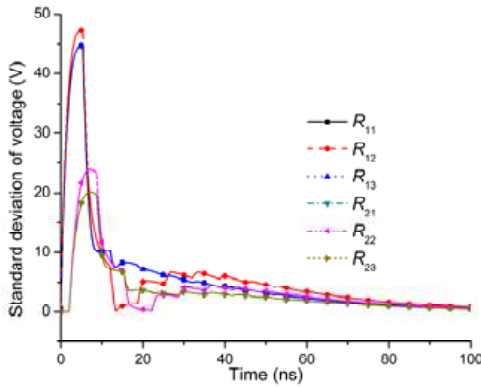


Figure 15. The standard deviations of the induced voltages in case 2 are estimated by the proposed method.

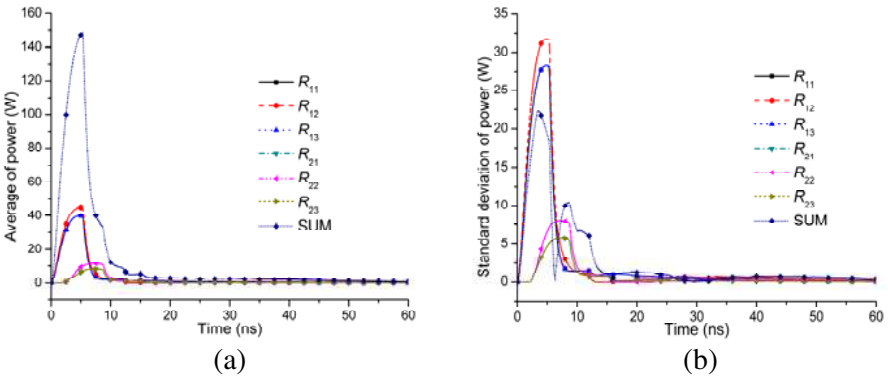


Figure 16. The averages and standard deviations of the induced powers in case 2 are estimated by the proposed method. (a) Averages. (b) Standard deviations.

powers in case 2 are estimated and shown in Figure 16, which agrees well with Figure 12.

5. CONCLUSIONS

This paper studies the effect of the bundle rotation on external fields coupling to the bundle and presents an efficient method to estimate the averages and standard deviations of the voltages and powers induced on the loads. The results show that both the real and imaginary parts of the induced voltages in the frequency domain and the transient induced voltages in the time domain are all sine functions of the rotation angle. The proposed estimation method, which needs only three times repeated calculations, can quickly provide the averages and standard deviations of the induced voltages and powers and the results agree well with those from statistical analysis.

ACKNOWLEDGMENT

Acknowledgement is made to National Natural Science Foundation of China for the support of this research through Grant No. 60971080.

REFERENCES

1. Taylor, C. D., R. S. Satterwhite, and C. W. Harrison, "The response of a terminated two-wire transmission line excited by a nonuniform electromagnetic field," *IEEE Trans. Antennas Propag.*, Vol. 13, No. 6, 987–989, 1965.
2. Agrawal, A. K., H. J. Price, and S. H. Gurbaxani, "Transient response of multiconductor transmission lines excited by a nonuniform electromagnetic field," *IEEE Trans. Electromagn. Compat.*, Vol. 22, No. 2, 119–129, 1980.
3. Rachidi, F., "Formulation of the field-to-transmission coupling equations in terms of magnetic excitation field," *IEEE Trans. Electromagn. Compat.*, Vol. 35, 404–407, 1993.
4. Paul, C. D., *Analysis of Multiconductor Transmission Lines*, Wiley, New York, 1994.
5. Erdin, I., A. Dounavis, R. Achar, et al., "A SPICE model for incident field coupling to lossy multiconductor transmission lines," *IEEE Trans. Electromagn. Compat.*, Vol. 43, No. 4, 485–494, 2001.
6. Haase, H., J. Nitsch, and T. Steinmetz, "Transmission-line super theory: A new approach to an effective calculation of

- electromagnetic interactions,” *URSI Radio Science Bull.*, No. 307, 33–60, 2003.
7. Tesche, F. M. and C. M. Butler, “On the addition of EM field propagation and coupling effects in the BLT equation,” *Interaction Note*, Vol. 588, 2004.
 8. Shinh, G. S., N. M. Nakhla, and R. Achar, “Fast transient analysis of incident field coupling to multiconductor transmission lines,” *IEEE Trans. Electromagn. Compat.*, Vol. 48, No. 1, 57–73, 2006.
 9. Cheldavi, A. and P. Nayeri, “Analysis of V transmission lines response to external electromagnetic fields,” *Progress In Electromagnetics Research*, Vol. 8, 297–315, 2007.
 10. Armenta, R. B. and C. D. Sarris, “Efficient evaluation of the terminal response of a twisted-wire pair excited by a plane-wave electromagnetic field,” *IEEE Trans. Electromagn. Compat.*, Vol. 49, No. 3, 698–707, 2007.
 11. Xie, H., J. Wang, R. Fan, et al., “A hybrid FDTD-SPICE method for transmission lines excited by a nonuniform incident wave,” *IEEE Trans. Electromagn. Compat.*, Vol. 51, No. 3, 811–817, 2009.
 12. Xie, H., J. Wang, R. Fan, and Y. Liu, “Spice models for radiated and conducted susceptibility analyses of multiconductor shielded cables,” *Progress In Electromagnetics Research*, Vol. 103, 241–257, 2010.
 13. Capraro, G. T. and C. R. Paul, “A probabilistic approach to wire coupling interference prediction,” *Proc. IEEE Int. Symp. Electromagn. Compat.*, 267–272, Zurich, Switzerland, 1981.
 14. Ciccolella, A. and F. G. Canavero, “Statistical simulation of crosstalk in Bundles,” *Pro. 11th Int. Zurich Symp. EMC*, 83–88, Zurich, Switzerland, 1995.
 15. Bellan, D., S. A. Pignari, and G. Spadacini, “Characterisation of crosstalk in terms of mean value and standard deviation,” *Proc. IEE Sci. Meas. Technol.*, Vol. 150, No. 6, 289–295, 2003.
 16. Wu, M., D. Beetner, T. Hubing, et al., “Estimation of the statistical variation of crosstalk in wiring harnesses,” *Proc. IEEE Int. Symp. Electromagn. Compat.*, 696–702, 2008.
 17. Sun, S., G. Liu, J. Drewniak, et al., “Hand-assembled cable bundle modeling for crosstalk and common-mode radiation prediction,” *IEEE Trans. Electromagn. Compat.*, Vol. 49, No. 3, 708–718, 2007.
 18. Beetner, D. G., H. Weng, M. Wu, et al., “Validation of worst-case and statistical models for an automotive EMC expert system,” *Proc. IEEE Int. Symp. on Electromagn. Compat.*, 2008.

19. Bellan, D. and S. A. Pignari, "Efficient estimation of crosstalk statistics in random wire bundles with lacing cords," *IEEE Trans. Electromagn. Compat.*, Vol. 53, No. 1, 209–218, 2011.
20. Stievano, I. S., P. Manfredi, and F. G. Canavero, "Stochastic analysis of multiconductor cables and interconnects," *IEEE Trans. Electromagn. Compat.*, Vol. 53, No. 2, 501–507, 2011.
21. Morgan, M. A. and F. M. Tesche, "Basic statistical concepts for analysis of random cable coupling problems," *IEEE Trans. Antennas Propag.*, Vol. 26, No. 1, 185–187, 1978.
22. Parkinson, E. R. and P. H. Levy, "Monte carlo analysis of the EMP response of a random-lay cable," *IEEE Trans. Nuclear Science*, Vol. 29, No. 6, 1920–1923, 1982.
23. Nuno, L. and C. L. Holloway, "Numerical investigation of the induced voltage on a cable placed at random locations inside a metallic enclosure," *Int. Symp. Electromagn. Compat. Europe*, 2008.
24. Paletta, L., J. P. Parmantier, F. Issac, et al., "Susceptibility analysis of wiring in a complex system combining a 3-D solver and a transmission-line network simulation," *IEEE Trans. Electromagn. Compat.*, Vol. 44, No. 2, 309–317, 2002.
25. Baum, C. E., T. K. Liu, and F. M. Tesche, "On the analysis of general multiconductor transmission-line networks," *Interaction Note*, Vol. 350, 1978.
26. Tesche, F. M., M. V. Ianoz, and T. Karlsson, *EMC Analysis Methods and Computational Models*, Wiley, New York, 1997.
27. Paul, C. R., "A SPICE model for multiconductor transmission lines excited by an incident electromagnetic field," *IEEE Trans. Electromagn. Compat.*, Vol. 36, No. 4, 342–354, 1994.